Mausam, (1996), **47**, 2, 133-144

551.533.21 : 551.515.1

Structure and properties of summer monsoon stationary wave over southern Asia : an observational study

SURANJANA SAHA
Development division, National Meteorological Center, NOAA
Washington, D. C., U. S. A.
and
K. R. SAHA
27, B-Road, Maharani Bagh, New Delhi
(Received 22 December 1994, Modified 3 July 1995)

सार — दक्षिणी एशिया तथा इसके समीपवर्ती महासागरीय क्षेत्रों की दस वर्ष (1976-1985) के जुलाई के औसत जलवायु विज्ञान के अध्ययन से, विभिन्न मौसमविज्ञानिक परिवर्तिताओं के क्षेत्र में, स्थल-समुद्र तापीय संकुचन का कारण माने जाने वाले एक सुपरिभाषित स्थायी प्रवाह की पुष्टि होती है। यह प्रवाह लगभग 20 डिग्री उत्तर में, 10 डिग्री पार्श्वीय विस्तार से अधिकतम तीव्रता के साथ तथा सतह से उर्ध्वाधरीय लगभग 300 एच०पी०ए० प्रवाहित होता है। इसका क्षेत्रीय तरंगदैर्ध्य लगभग 2000-2500 कि०मी० है और तापमान की क्षेत्रीय अनियमितता में इसका विस्तार तथा दक्षिणीय वायु के घटक, क्रमशः 1 डिग्री सेल्सियस और 4 मी०/से० हैं। द्रोणी-कटक प्रणाली सतह से लगभग 700 एच०पी०ए० ऊँचाई के साथ प्रवाह पूर्व की ओर मुड़ती प्रतीत होता है और पश्चिम की तरफ लगभग 300 एच०पी०ए० ऊपर चढ़ती है। जबकि उष्ण-शीत अनियमितता में सतह से लगभग 300 एच०पी०ए० पूर्व की ओर यह मुड़ती प्रतीत होता है। निम्न तथा उच्च दोनों ही क्षोभ मंडलीय तापमान क्षेत्रों में भू-विभव के मध्य एक कालांतर प्रतीत होता है मानसून द्रोणी का उक्त क्षेत्रीय उर्ध्वाधरीय भंवर तथा भू-विभव एवं तापमान क्षेत्रों के मध्य कालांतर संगत प्रतीत होता है। पश्चिम पूर्व (दक्षिणावर्त) अपवर्तन के साथ पूर्व की तरफ रुख वाले निम्न क्षोभमंडलीय द्रोणी के मामले में पश्चिम में उठने वाली उष्ण हवा तथा पूर्व में ठहरने वाली शीत हवा तथा पूर्व-पश्चिम (वामावर्त) अपवर्तन के साथ पश्चिम की तरफ रुख वाले मध्य और ऊपरी क्षोभमंडलीय द्रोणी के मामले में पूर्व में उठने वाली उष्ण हवा तथा पश्चिम में ठहरने वाली शीत हवा से गुजरकर तापीय अभिवहन के माध्यम से भंवर-जनित विभव ऊर्जा, भंवर गतिक ऊर्जा में सीधे परिवर्तित होती है। तापीय अभिवहन में वृद्धि तथा उसके कारण उर्ध्वाधर परिचालन से कभी-कभी निम्न दाब अथवा अवदाब में द्रोणी बन सकती है। तथापि, द्रोणी के बनने तथा इसके विकास में सहायक भौतिक कारकों की जाँच इस संबंध में और अधिक अध्ययन द्वारा ही सम्भव है।

ABSTRACT. A study of ten-year (1976-1985) mean July climatology of southern Asia and adjoining ocean areas confirms the presence of a well-defined stationary wave believed to be due mainly to land-sea thermal contrast over the region, in the fields of several meteorological variables. The wave extends laterally over about 10 degrees of latitude with maximum intensity along about 20° N and vertically from surface to about 300 hPa. Its zonal wavelength is about 2000-2500 km and its amplitude in the field of zonal anomaly of temperature and meridional component of wind is 1°C and 4ms^{-1} respectively. The trough-ridge system of the wave appears to tilt eastward with height from surface to about 700 hPa and westward aloft up to about 300 hPa, while the warmest-coldest anomaly system appears to tilt eastward all the way from surface to about 300 hPa. A phase difference appears to exist between the geopotential and the temperature fields in both the lower and the upper tropospheres. The aforesaid zonal-vertical tilt of the monsoon trough and phase difference between the geopotential and the temperature fields appears to be compatible, through thermal advection, with a direct conversion of eddy available potential energy into eddy kinetic energy *via* a west-east (clockwise) overturning with warm air rising in the west and cold air sinking in the east in the case of the eastward-tilting lower-tropospheric trough and an east-west (anti-clockwise) overturning with warm air rising in the east and cold air sinking in the west in the case of the westward-tilting middle and upper-tropospheric trough. An enhancement of the thermal advection and hence the vertical circulation may occasionally lead to development of the trough into a low or depression. However, the question of development of the trough and physical factors, which may contribute to such development, needs to be examined by further study.

Key words — Monsoon stationary wave, Structure of stationary wave, Properties of stationary wave, Stationary wave, Monsoon depressions.

1. Introduction

A first comprehensive study of the surface wind field over the Indian Ocean and the western Pacific led Fu *et al.* (1983) to discover the presence of a wave-like structure at the southern periphery of the huge summer low pressure over the Asian continent. As part of this wave, they found three low pressure troughs over the eastern edges of Africa, India and Indo-China peninsula, which controlled the three main branches of the southwest monsoon, one each over the Arabian Sea, the Bay of Bengal and South China Sea and influenced the rainfall pattern in south Asia. It appears that the stationary

TABLE 1

Mean standard deviation of monthly mean values of different parameters from their climatological mean for July at 850, 500 and 200 hPa

Pressure (hPa)	Temperature (°C)	Windspeed (ms^{-1})		Dewpoint (°C)
		u	v	
850	1.02 (91)	1.52 (107)	1.48 (107)	1.31 (105)
500	0.82 (111)	2.11 (110)	1.66 (109)	2.00 (115)
200	1.19 (107)	4.06 (108)	3.24 (107)	Not computed

character of the monsoon wave was well recognized by these workers in that they found the wave corresponded to perturbations of the temperature field in the lower troposphere caused by land-sea thermal contrast in the area. Unfortunately, there has been little follow-up study of this important finding and several questions relating to the detailed structure and properties of this wave and its relationship with the prevailing weather over the region still remain. For example, we do not yet adequately know the horizontal and vertical extent of this wave and how it manifests itself in different meteorological fields, such as, wind (or geopotential), temperature, moisture and rainfall. We need detailed information regarding the vertical structure of the trough-ridge system in relation to the thermal structure in order to address the question of development. For, it is common knowledge that most of the summer monsoon lows and depressions develop in the monsoon trough zone which constitutes an integral part of the stationary wave. What is the mechanism of this development and what physical factors are involved in it? Obviously, further studies are required to address some of these questions. The present observational study may be said to be an attempt in this direction.

There has been a controversy in the past regarding the relative roles of land-sea thermal contrast and mountains in the formation and maintenance of the monsoon stationary wave. While Holopainen (1970), from an observational study of the energy balance of the stationary distrubances over the globe, concluded that the contribution of the mountains is likely to be negligible compared to that of the land-sea thermal contrast during the northern summer, some theoretical and numerical studies (*e.g.*, Banerji 1930, Hahn and Manabe 1975) have stressed the importance of the mountain effect, especially in the region of the Himalayas. However, in the present study, we did not address this question.

The layout of the paper is as follows :

Section 2 introduces data, analysis and computations. Section 3 traces the wave structure in various meteorological fields. An idealized model of the stationary wave showing the vertical structure of its trough-ridge system and temperature anomalies is presented in section 4. Main findings of the study are summarized in section 5.

2. Data, analysis and computations

The study utilizes a ten-year (1976-85) mean July climatological data set consisting of wind, temperature and dew-point at surface and isobaric surfaces 850, 700, 500, 300, 200, 100 and 50 hPa over Asia and adjoining ocean areas bounded by latitudes 0° and 55°N and longitudes 35° and 125°E. The data set also includes mean July rainfall over the area. The rationale behind selecting the period 1976-85 for the climatology was maximization of available data in space and time. There was large-scale expansion of data network around 1979 when the Global Weather Experiment was carried out with a strong component of Monsoon Experiment (MONEX) over the Indian Ocean and western Pacific. It was also during this period that data from mainland China including Tibet became available for a few years at a stretch, after a gap of several years. The sources of data include : (i) Monthly Climatic Data of the World published by the United States of America Department of Commerce; (ii) Special MONEX Datasets published by the International MONEX Management Center (IMMC) and available with the India Meteorological Department (IMD) at its Headquarters at New Delhi; (iii) Regional Daily/Monthly Weather Reports published by the IMD and (iv) Mausam (formerly Indian Journal of Meteorology, Hydrology and Geophysics) also published by the IMD. We also utilized a data set relating to the period (1963-66) of the International Indian Ocean Expedition (IIOE), published by Ramage and Raman (1972).

The coverage and quality of data was generally good over the land, barring mountainous regions where data were sparse, but not quite so over the oceans where, as usual, there were large data holes. The total number of reporting stations included in the climatology is around 185, distributed rather unevenly over the region, with the maximum (53)

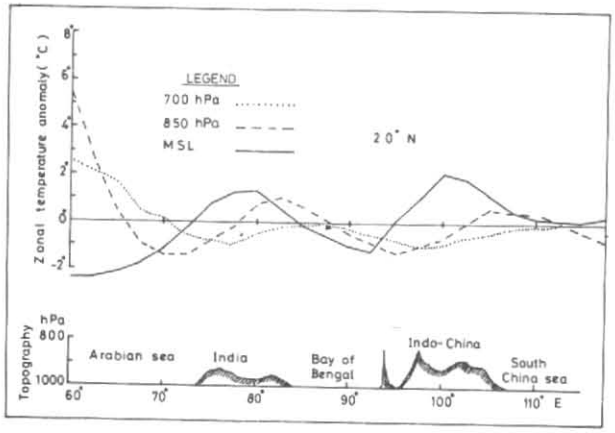

Fig. 1. Zonal anomaly of temperature (°C) at MSL (continuous), 850 hPa (dashed) and 700 hPa (dotted) along 20°N. Topography and land-sea distribution are shown at bottom. Positive-Warm, Negative-Cold

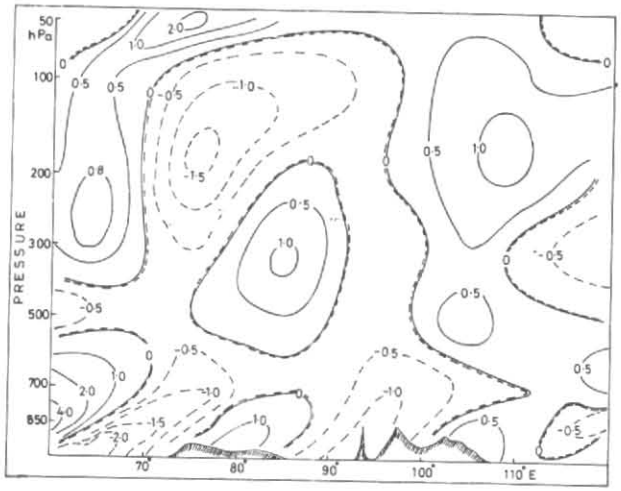

Fig. 2. Vertical section of zonal anomaly of temperature (°C) along 20°N. Positive-Warm, Negative-Cold

between 20° and 30°N which is predominantly land and mimimum (20) between the equator and 10°N which is largely ocean. Unfortunately, some stations' data were missing in some years, so the time-averaging at these stations could be done for a period less than ten years. This is likely to introduce an element of inhomogeneity in the climatology which is, perhaps, unavoidable. A measure of interannual variability of the different parameters is furnished in Table 1 which gives the standard deviation of their mean July values about the climatological mean at three standard pressure surfaces 850, 500 and 200 hPa, averaged over the number of reporting stations shown in parenthesis. Generally speaking, the interannual variability of wind and dew-point increases with height, while in the case of temperature it is less at 500 hPa than at 850 or 200 hPa.

The main objective of the analysis was to secure a description of the fields of the different variables at pressure surfaces. For this purpose, data were plotted on standard isobaric maps and analyzed manually, following standard procedures. Temperatures at surface over land were reduced to mean sea level (MSL) and/or standard isobaric surfaces below the station level by assuming a standard lapse rate of 6.5°C per km. In the case of winds, they were first resolved into the eastward (u) and the northward (v) components at each pressure surface and then analyzed like any other scalar variable. Moisture analysis aimed at securing the fields of humidity-mixing-ratio, computed from values of temperature and dew-point, at each pressure surface upto 300 hPa. From the analysis, grid-point values were picked up at 2.5° lat./long. intervals for further study and computations.

Parameters computed from the basic data included horizontal divergence of wind, vorticity, vertical motion, horizontal thermal advection and diabatic heating. Vertical velocity was computed using the well-known continuity equation with orographic lifting velocity as the lower boundary condition. Diabatic heating was computed as a residual from the first law of thermodynamics. The formulae used for the computations are (unless otherwise stated, the basic parameters used in the computations are all time-mean values):

Zonal anomaly X' of parameter X,

$$X' = X - [X] \tag{1}$$

Meridional anomaly X'' of parameter X,

$$X'' = X - \langle X \rangle \tag{2}$$

Horizontal divergence,

$$D = \partial u/\partial x + \partial v/\partial y - (v/a)\tan\phi \tag{3}$$

Relative vorticity,

$$\zeta = \partial v/\partial x - \partial u/\partial y + (u/a)\tan\phi \tag{4}$$

Vertical motion at p-surface,

$$\omega_p = \omega_s + \int_p^{p_s} \bar{D}\,\delta p \tag{5}$$

Diabatic heating,

$$Q = (C_p/g) \int_{p_T}^{p_s} (\bar{u}\partial\bar{T}/\partial x + \bar{v}\partial\bar{T}/\partial y - \bar{\sigma}\bar{\omega})\delta p \tag{6}$$

where, the rectangular bracket [ ] and the angular bracket < > denote respectively the zonal and the

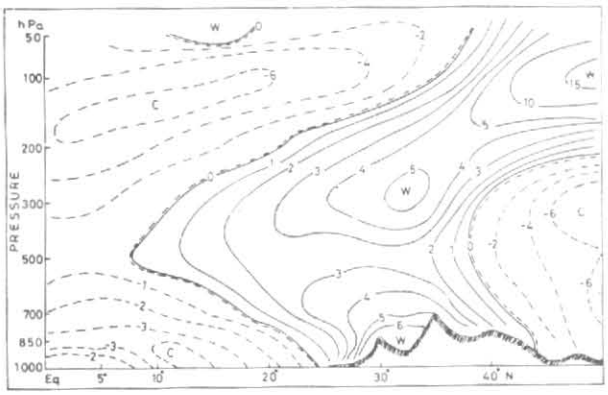

Fig. 3. Vertical section of meridional anomaly of temperature (°C) along 70° E. Positive-Warm, Negative-Cold

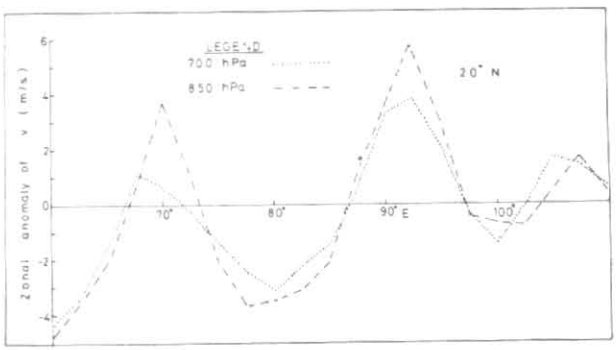

Fig. 4. Zonal anomaly of meridional component of wind (v) in ms^{-1} at 850 hPa (dashed) and 700 hPa (dotted) along 20° N. Positive-Southerly, Negative-Northerly

meridional average, the overbar an average over a pressure interval δp, α the radius of the earth, ϕ the latitude, C_p the specific heat of air at constant pressure, g the acceleration due to gravity, ω_s the vertical p-velocity at the lower boundary surface at pressure p_s, p_T the pressure at the top of the domain, T the absolute temperature and σ the static stability parameter. In the expression for diabatic heating (6), the time-mean value of a term, $\partial T/\partial t$ (temperature tendency) is neglected.

3. Wave structure in meteorological fields

The presence of a stationary wave in the monsoon atmosphere over southern Asia is revealed by the spatial distribution of the time-mean values, or the zonal or meridional anomalies, of temperature, wind, moisture and rainfall as well as some of their derived properties, such as, divergence, vorticity, vertical motion, diabatic heating and circulation. In what follows, a brief account is presented of some of these distributions.

(*a*) *Temperature field*

Fig. 1 shows the longitudinal distribution of zonal anomaly (deviation from zonal mean) of temperature at MSL, 850 and 700 hPa along 20° N. It brings out the land-sea thermal contrasts with the warm sectors generally appearing over the land and the cold sectors over the sea. There appears to be a general eastward shift of the temperature maxima and minima with height over both land and sea. A fuller view of the structure of the wave is furnished in Fig. 2 which shows the vertical distribution of the zonal temperature anomaly along 20° N through the whole atmosphere upto about 50 hPa. Land-sea thermal contrast and zonal-vertical profiles of the warm and cold sectors are more clearly seen here. Fig. 2 would seem to suggest that the stationary wave is basically a phenomenon of the lower atmosphere with its upper boundary somewhere close to 500 hPa. Its wave-length in the temperature field would appear to be around 2500 km and the thermal amplitude is about 1°C. Above about 500 hPa, the structure of the temperature wave appears to change considerably, as it comes under the influence of the upper-tropospheric warm high over Asia which forms part of planetary-scale monsoon with wave number 1 to 2 in the zonal direction. A detailed analysis of the planetary-scale monsoon wave at 200 hPa was presented by Krishnamurti and Kanamitsu (1977). A characteristic feature of the thermal structure above 500 hPa (Fig. 2) is a pronounced secondary temperature maximum (warm anomaly) situated over the low-level temperature maximum over the land and a minimum (cold anomaly) over the low-level temperature minimum over the sea. Features similar to those in Fig. 2 were also found along 15° and 25° N but not along 10° or 30° N. The meridional domain of the wave would, therefore, appear to extend from about 15° to about 25° N with the strongest intensity along about 20° N.

Fig. 3, which gives the vertical distribution of meridional anomaly (deviation from meridional mean) of temperature along 70° E, confirms the presence of a mid-tropospheric temperature maximum (minimum) above the lower-tropospheric temperature maximum (minimum) over the land (sea). Features similar to those presented in Fig. 3 were also found in meridional-vertical sections along 90° and 110° E.

(*b*) *Wind field*

The analysis of the wind field was done separately for u and v components. The u-field revealed

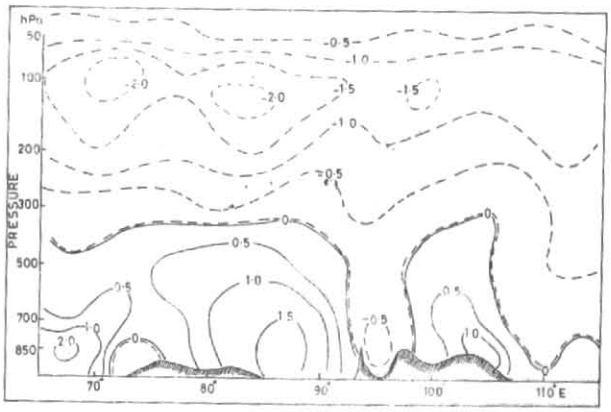

Fig. 5. Distribution of relative vorticity (unit : 10^{-5} s^{-1}) in vertical section along 20°N. Positive-cyclonic. Negative-anticyclonic

the well-known features of zonal circulation over the region with westerlies below and easterlies above. The depth of the westerlies increased from the trough location equatorward and attained a height of about 6 km along about 10°N. The easterlies prevailed above about 500 hPa and were strongest over the latitudes of southern India at an altitude of about 150 hPa.

The longitudinally averaged *v*-field over southern Asia shows a general poleward flow from sea to land in the lower troposphere and a reverse equatorward flow aloft. However, as shown in Fig. 4, a distinct wave pattern can be seen in the zonal anomaly of the *v*-component at 850 and 700 hPa along 20°N. Between the northerly and the southerly flows at both the surfaces the locations of three monsoon troughs, one each over the eastern part of the Arabian Sea, the western part of head Bay of Bengal and the western part of South China Sea can be identified. The mean zonal wave-length and amplitude of the wave in the *v*-field would appear to be about 2000-2500 km and 4 ms^{-1} respectively.

(*c*) *Relative vorticity* (ξ)

Fig. 5 presents the distribution of relative vorticity in a zonal-vertical section along 20°N. It reveals alternate segments of positive and negative relative vorticity, reflecting the stationary wave character of monsoon flow below about 400 hPa.

We also examined the distributions of relative vorticity in two meridional-vertical sections along longitudes 77.5° and 85°E with a view to finding the meridional slope of the monsoon trough with height, assuming that the positive relative vorticity would be maximum at the trough location. The

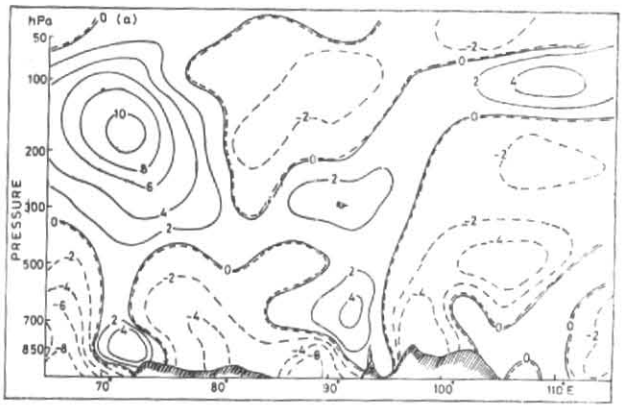

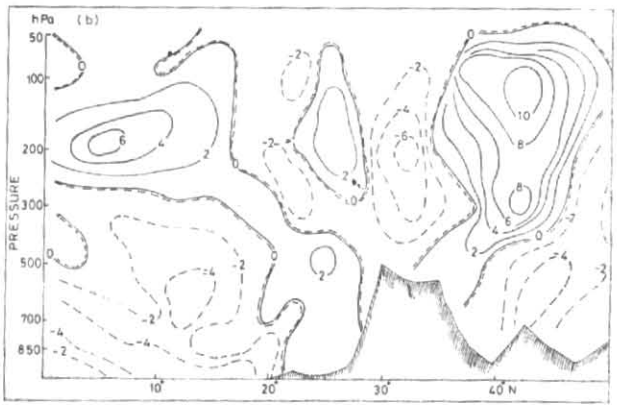

Figs. 6 (a & b). Distribution of divergence (unit : 10^{-6} s^{-1}) in vertical sections along (a) 20°N and (b) 85°E. Positive-divergence. Negative-convergence

results (not presented for lack of space) show that along 77.5°E which passes through the western part of the trough, the slope is distinctly equatorward with an angle of about 1/100, while along 85°E which passes through the eastern part, the trough is almost vertical upto about 600 hPa, above which it tilts rapidly equatorward.

(*d*) *Divergence* (*D*)

Figs. 6(a & b) present the vertical distributions of horizontal divergence along 20°N [Fig. 6 (a)] and 85°E [Fig. 6 (b)] respectively. The section along 20°N [Fig. 6 (a)] shows convergence in the lower troposphere with divergence aloft over the eastern part of the Arabian Sea (except the coastal belt), the Indian peninsula and adjoining Bay of Bengal between about 76° and 92°E, the Indo-China peninsula mountains and South China Sea east of about 110°E. Low-level divergence appears over a narrow belt of longitudes off the west coast of India, the eastern part of the Bay of Bengal and a broad belt of longitudes over South China Sea between the coast of Indo-China and longitude about 110°E.

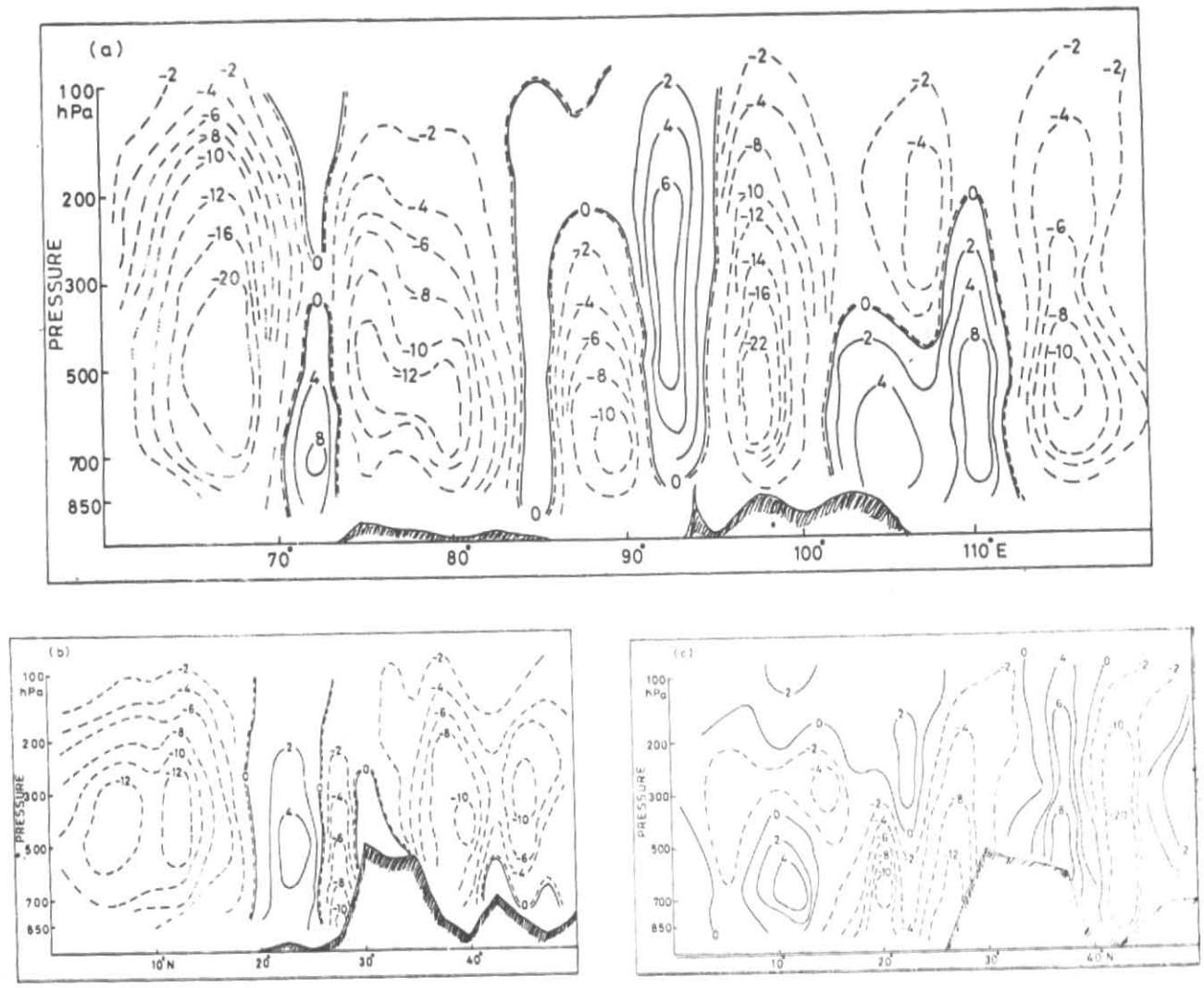

Figs. 7 (a-c). Distribution of vertical velocity (unit : 10^{-4} hPa s^{-1}) in vertical sections along (a) 20°N, (b) 85°E and (c) 90°E. Positive-Downward, Negative-Upward

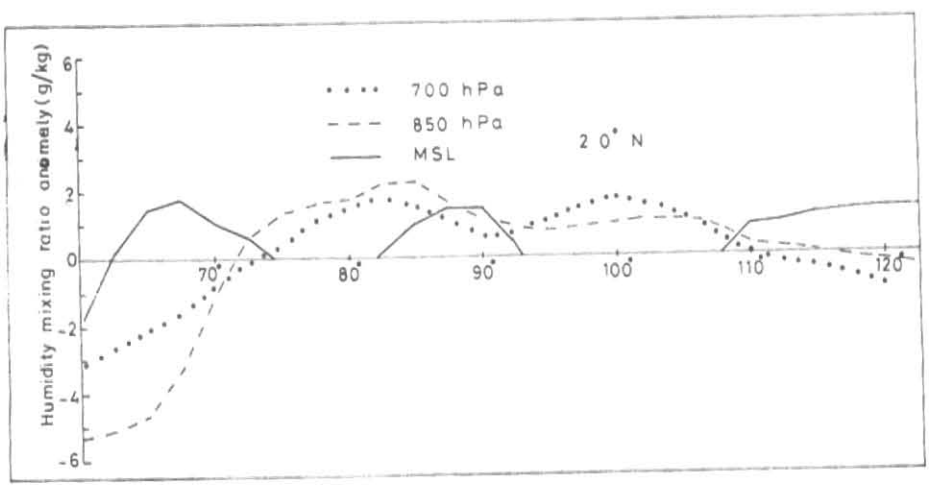

Fig. 8. Zonal anomaly of humidity mixing ratio (g/kg) at MSL (continuous), 850 hPa (dashed) and 700 hPa (dotted) along 20°N

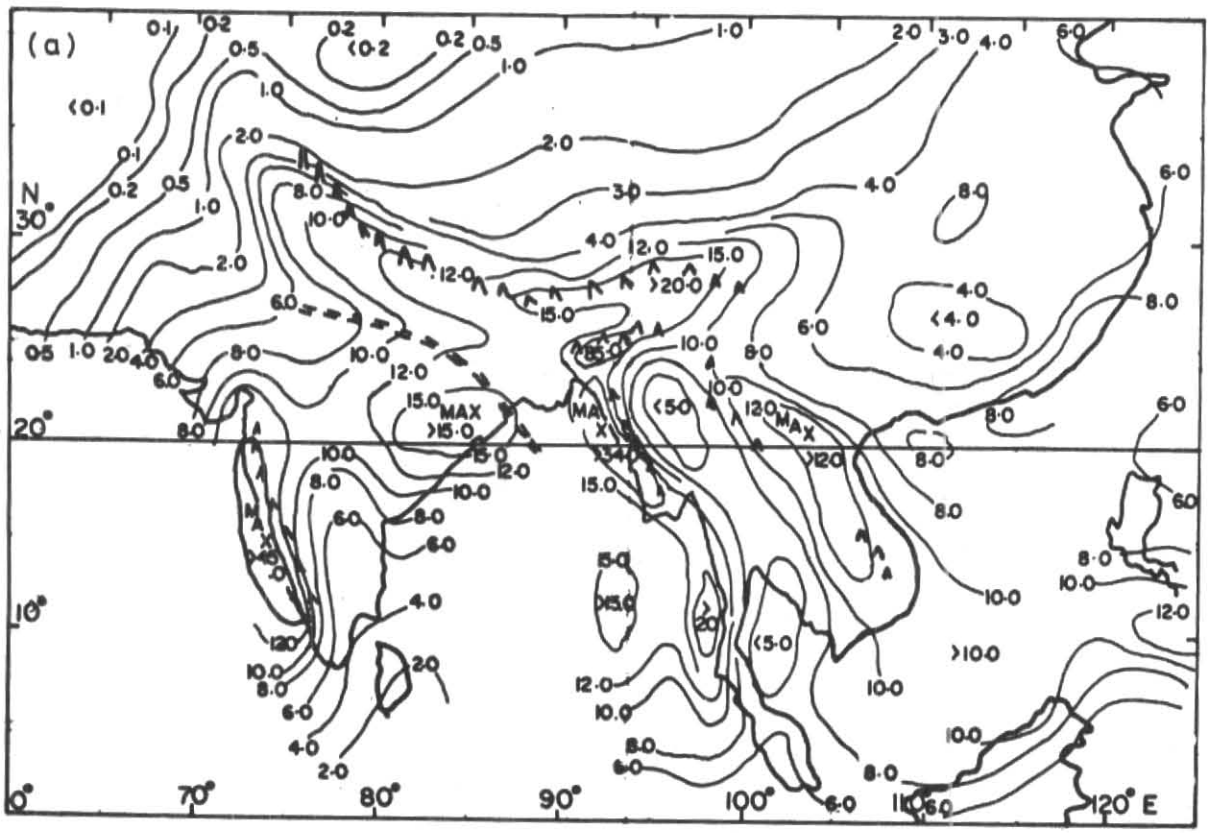

Fig. 9 (a). Distribution of ten-year (1976-85) mean July rainfall (unit : 10^{-5} kg s^{-1} m^{-2}) for the Southern Asia

The section along 85°E [Fig. 6 (b)] reveals lower-tropospheric convergence with divergence aloft over a broad belt of latitudes from the equator to about 21°N and divergence to the north over the plains of northern India. However, covergence appears along the slopes of the Himalayas above about 700 hPa. In the upper troposphere over the Tibetan plateau, strong convergence appears between about 300 and 100 hPa with a maximum at about 200 hPa.

(*e*) *Vertical motion* (ω)

Field of vertical motion consistent with the distribution of divergence and convergence in the monsoon-atmosphere are shown in two vertical sections, zonal [Fig. 7 (a)] along 20°N and meridional [Fig. 7 (b)] along 85°E. In Fig. 7 (a), alternate segments of upward and downward motions appear, reflecting the stationary wave character of the monsoon flow. Since meridian 85°E lies somewhat westward of the location of the monsoon trough at MSL, Fig. 7 (c) presents the meridional-vertical section of vertical motion along 90°E which lies somewhat to the east of the trough. The difference between the patterns of vertical motion along the two longitudes appears to be well-marked. Along 85°E [Fig. 7 (b)], there is strong downward motion over the plains of northern India, whereas along 90°E [Fig. 7 (c)] there is upward motion all over the plains extending right up to the Himalayas.

(*f*) *Moisture field*

Since surface evaporation is maximum over the sea and minimum over the land, a wave pattern reflecting this land-sea contrast in moisture content at MSL is well evident in Fig. 8 which presents the zonal anomaly of humidity-mixing-ratio at MSL, 850 and 700 hPa along 20°N. However, as may be seen from Fig. 8, the moisture content falls off with height much more rapidly over the sea than over the land with the result that at 850 and 700 hPa the atmosphere over the land holds much more moisture than that over the sea. It is likely that low-level convection over land and subsidence over sea may play a crucial role in creating this type of moisture distribution.

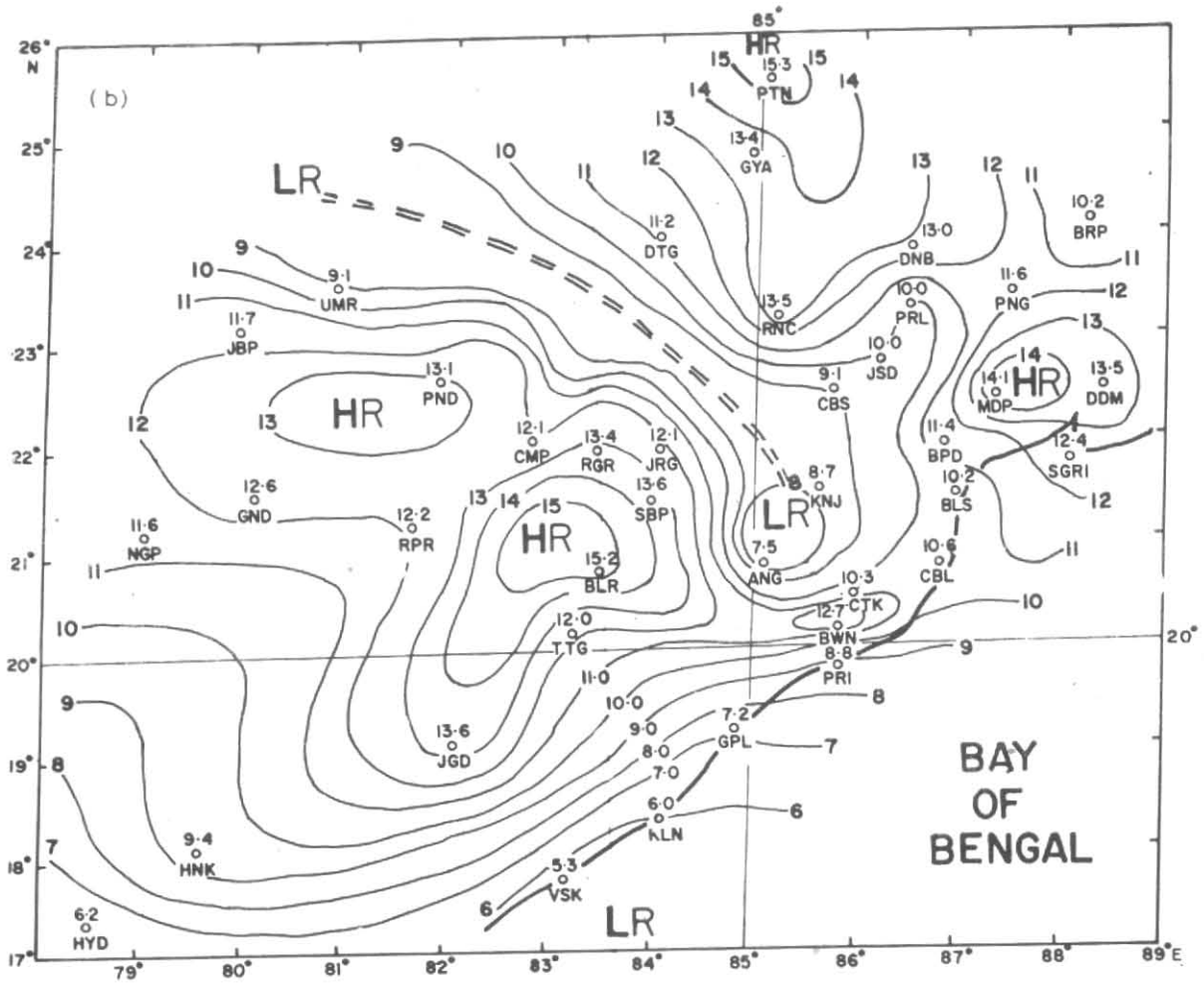

Fig. 9 (b). Distribution of ten-year (1976-85) mean July rainfall (unit : 10^{-5} kg s^{-1} m^{-2}) for the central and eastern India. HR denotes Heavy rain, LR Light rain

(g) *Rainfall field*

Fu *et al.* (loc. cit.) stressed the importance of the branching phenomenon of the southwest (SW) monsoon to account for the observed rainfall pattern over southern Asia. But the rainfall they refer to is the orographic rainfall at the west coasts of India and Indo-China peninsulas. Undoubtedly, there are heavy concentrations of orographic rain along each of the branches of the SW monsoon which lie to the east of a monsoon trough, as pointed out by these workers, but one can also see in Fig. 9 (a), which presents the ten-year mean July rainfall distribution over southern Asia, an area of heavy rainfall to the west/southwest of the trough over eastern India which can not possibly be attributed to orography. A detailed meso-scale analysis of the rainfall pattern relative to the monsoon trough over central and eastern India was, therefore, carried out and the result is presented in Fig. 9 (b). It shows a rainfall minimum at the trough location flanked by rainfall maxima over central India in the west and plains of northeastern India and the slopes of the Himalayas in the east. Similar pattern of rainfall in relation to monsoon trough may also be found over southeastern China bordering South China Sea.

(h) *Diabatic heating*

The first law of thermodynamics, as applied to the atmosphere, represents the adiabatic response of the atmosphere to any diabatic heating or cooling. Unfortunately, it is difficult to measure diabatic heating or cooling directly in the atmosphere in the absence of requisite data. However, it is possible to measure the terms on the right hand side of equation (6) which constitute the adiabatic response in terms of atmospheric circulation features to obtain diabatic heating indirectly.

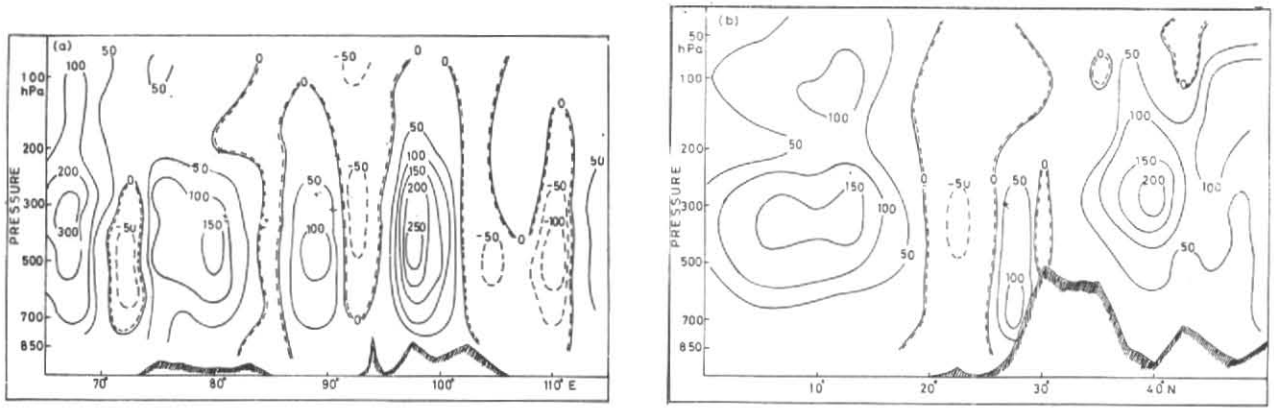

Figs. 10 (a & b). Distribution of diabatic heating (unit : W m^{-2}) in vertical sections along (a) 20°N and (b) 85°E

Results of computation of diabatic heating using (6) are presented in two vertical sections, *viz.*, one zonal along 20°N [Fig. 10 (a)] and the other meridional along 85°E [Fig. 10 (b)]. In Fig. 10 (a), alternate segments of heating (positive values) and cooling (negative values) appear reflecting the stationary wave character of the field of diabatic heating. Broad positive segments appear westward of the location of the monsoon trough over India, while a negative segment appears at the trough location itself. In the South China Sea sector, two negative segments would seem to be present, one near 105°E and the other near 110°E, the two being separated in the upper troposphere by a positive segment. In Fig. 10 (b), diabatic heating appears to the south of about 20°N and along the slopes of the Himalayas while diabatic cooling prevails over the plains of northern India. In the absence of adequate data, it is not easy to interpret the net diabatic heating or cooling in the atmosphere. It could be the result of several physical processes, such as, release of latent heat due to precipitation, radiative heat loss caused by longwave radiation, sensible and latent heat fluxes across the boundary, etc. However, in the free atmosphere, the net diabatic heating or cooling is largely determined by the relative values of precipitation heating and radiative cooling. In areas where there is a precipitation minimum, such as at the monsoon trough location, radiative heat loss may dominate over precipitation heating and the result may be a net diabatic cooling. On the other hand, in areas where there is large-scale heavy precipitation, such as that lying to the southwest of the monsoon trough, latent heat released by precipitation may dominate over radiative heat loss and there may be a net diabatic heating of the atmosphere. The distribution of net diabatic heating (cooling) appears to be well correlated with upward (downward) motion in the atmosphere.

(*i*) *Circulation*

It is well-known that the magnitude of vertical motion (ω) is almost two to three orders of magnitude smaller than that of horizontal motion (u, v) in the atmosphere. Despite this difference in magnitude, it may be possible to combine the two, by ignoring the difference in scale, to produce what may be called approximate resultant streamlines in zonal-vertical or meridional-vertical planes. Results of an attempt made to produce such streamlines are presented in Figs. 11 (a & b) for vertical sections along 20°N and 85°E respectively.

The zonal section along 20°N [Fig. 11 (a)] shows broad streams of westerlies below about 500 hPa and easterlies aloft. The two streams appear to be rising and falling at places and between them produce anti-clockwise circulation cells centered at some heights above the surface. From west to east, the cell over the west coast of India appears to be centered between 500 and 300 hPa but those over the east coast of India and the west coast of Myanmar lie between 700 and 500 hPa. The cell over the South China Sea appears to be centered between 850 and 700 hPa. Fig. 11 (b), the meridional section along 85°E reveals strong subsidence over the monsoon trough zone with the upper-tropospheric northerlies descending steeply between about 25° and 20°N but rising along the southern slopes of the HImalayas and also over a broad belt of latitudes south of the trough zone. Between the location of the monsoon trough and the Himalayas, one can discern an anti-clockwise circulation cell centered at latitude about 26°N between 300 and 200 hPa. Such a circulation cell was found by Saha and Saha (1989) using another data set (1963-66) and called a 'mountain cell'.

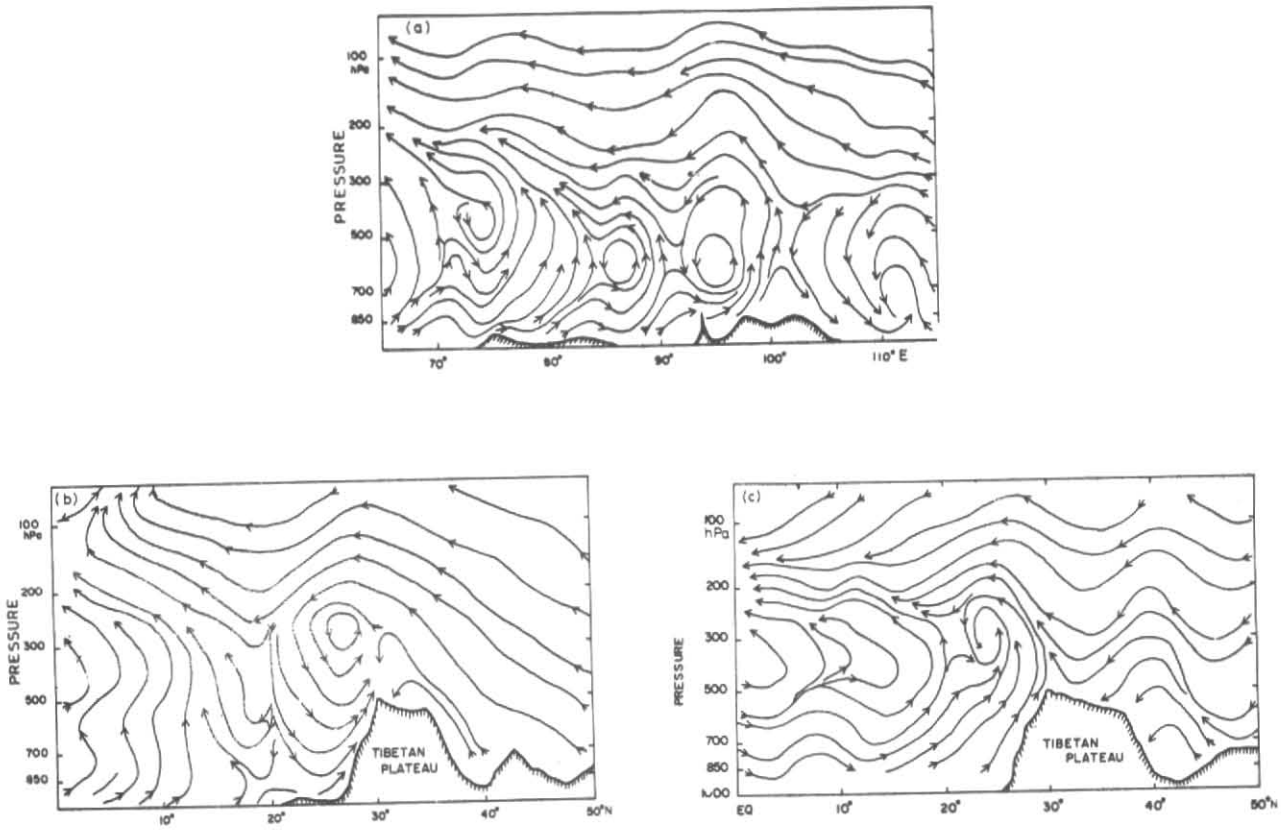

Figs. 11 (a-c). Approximate resultant streamlines in vertical sections along : (a) 20°N, (b) 85°E and (c) 90°E

Since the meridian 85°E lies to the west of the monsoon trough over India along 20°N at MSL, it may be of interest to examine the approximate streamlines in a meridional-vertical section along 90°E which lie somewhat to the east of the trough, shown in Fig. 11 (c). The difference in the pattern of circulation between the two meridians appears to be very striking. Whereas, the upper-tropospheric northerlies descend to very low levels along 85°E, they dip only slightly along 90°E, with the result that the 'mountain cell' is more prominent in the former than in the latter. Along 90°E, southerlies blow all the way from the equatorial region to the mountains with strong rising motion along the slopes of the Himalayas, though the 'mountain cell' is less marked.

4. An idealized model

Several details of the structure of the monsoon stationary wave presented in the foregoing section can now be placed together to construct an idealized model of the wave in the geopotential (or wind) and the temperature fields in space. Such a model is presented in Fig. 12 which shows the trough-ridge system in relation to the warmest-coldest anomalies at two pressure surfaces (300 and 850 hPa) and in a zonal-vertical section along 20°N, as estimated from the present data set and an earlier 4-year (1963-66) mean July data set (Ramage and Raman 1972) for the same region. The reason for using the earlier data set was that it contained the geopotential height data which were not included in the present data set. In using the additional data set, it was ensured that the temperature and wind fields which were associated with the height field were more or less identical in the two sets.

Fig. 12 would appear to bring out the following salient features :

(*i*) There exists a phase difference between the geopotential and the temperature fields so that the warmest (coldest) anomaly lags behind the geopotential trough (ridge), looking downstream, in both the lower (below about 700 hPa) and the upper (between about 500 and 300 hPa) troposphere. As mentioned earlier, the prevailing wind is westerly

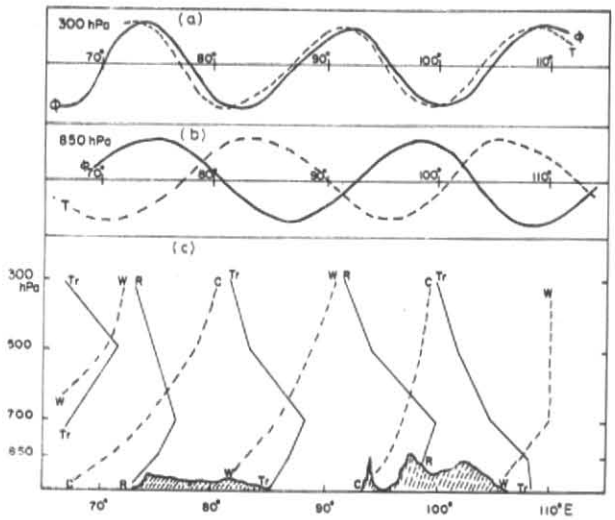

Figs. 12 (a-c). An idealized model of the monsoon stationary wave showing the distribution of the trough-ridge system relative to the coldest-warmest anomalies at (a) 300 hPa, (b) 850 hPa and (c) in a zonal-vertical section, along 20°N. ϕ denotes geopotential, T-temperature, C-cold, W-warm, R-ridge and Tr-trough

(easterly) in the lower (upper) troposphere. Over the eastern Arabian Sea, the warmest anomaly and its associated trough appears to be lifted from surface and mostly in the mid-troposphere.

(*ii*) The trough-ridge system appears to tilt eastward with height in the lower troposphere upto about 700 hPa (500 hPa over the eastern Arabian Sea) and westward aloft up to about 300 hPa, while the warmest-coldest anomaly system tilts eastward with height all the way upto 300 hPa. However, over South China Sea sector, the trough appears to tilt westward all the way from surface upward, although the warmest anomaly tilts somewhat eastward with height up to about 700 hPa and then remains almost vertical aloft.

(*iii*) At about 300 hPa, the geopotential and the temperature waves would appear to be in phase so that the trough (ridge) coincides with the coldest (warmest) anomaly.

The existence of a phase difference between the geopotential and the temperature fields and an eastward tilt of the monsoon trough with height in the lower troposphere and their significance in the context of the maintenance of the trough and its possible further development into a low or depression, was discussed earlier by Saha and Chang (1983). In the idealized model presented in Fig. 12, the vertical tilt of the monsoon trough and the phase difference between the geopotential and the temperature fields in the lower as well as the upper troposphere would, through thermal advection, lead to a direct conversion of eddy available potential energy into eddy kinetic energy via a west-east (clockwise) overturning with warm air rising in the west and cold air sinking in the east in the lower troposphere and an east-west (anti-clockwise) overturning with warm air rising in the east and cold air sinking in the west in the middle and upper troposphere. It is likely that the trough of the monsoon stationary wave, where the positive relative vorticity is maximum, is maintained by such a direct energy conversion process. It is also likely that an enhancement of the aforesaid energy conversion process may occasionally lead to the development of the trough into a low or depression. However, the question of possible further development of the trough and the mechanism which may lead to it requires further study.

5. Conclusions

The findings of the present study may be summarized as follows :

(*i*) A stationary wave which appears to owe its existence primarily to land-sea thermal contrast over the region of southern Asia manifests itself in several meteorological fields, such as, temperature, geopotential, wind, moisture and rainfall.

(*ii*) The horizontal north-south extent of the wave appears to be about 10 degrees of latitude from 15° to about 25°N with maximum intensity along about 20°N. Vertically, the wave extends from surface to about 300 hPa. Its average zonal wave length appears to be about 2000-2500 km and amplitude about 1-2°C in the temperature field and about 4 ms^{-1} in the v-field.

(*iii*) There appears to be a phase difference between the geopotential (or the wind) and the temperature fields in both the lower troposphere (below about 700 hPa) where the prevailing wind is westerly and the middle and upper troposphere where the prevailing wind is easterly. The temperature wave appears to lag behind the geopotential wave, looking downstream.

(*iv*) The trough-ridge system of the wave appears to tilt eastward with height from surface to about 700 hPa and westward aloft, while the warmest-coldest anomaly system tilts eastward practically at all heights. This allows warm

advection to the trough zone from the west at low levels and the east aloft.

(*v*) The stationary wave appears to be associated with several features of observed monsoon activity over the region, such as, large-scale convection, diabatic heating and cooling, orographic and non-orographic rainfall, etc.

(*vi*) The stationary wave appears to be maintained by a direct conversion of eddy available potential energy into eddy kinetic energy *via* a west-east (clockwise) overturning with warm air rising in the west and cold air sinking in the east in the lower troposphere and an east-west (anti-clockwise) overturning with warm air rising in the east and cold air sinking in the west in the middle and upper troposphere. An enhancement of this energy conversion process may occasionally lead to development of the trough into a low or depression. However, the question of possible development of the trough requires further study.

Acknowledgement

The authors express their grateful thanks to the Director General of Meteorology, India Meteorological Department, New Delhi, for several facilities extended during preparation of this paper. They also thank an anonymous reviewer for his helpful and constructive comments and suggestions on a first draft of the paper.

References

Banerji, S. K., 1930, "The effect of the Indian mountain ranges on air motion", *Ind. J. Phys.*, **5**, 699-745.

Fu, C. B., J. Fletcher and Slutz, R., 1983, "The structure of the Asian monsoon surface wind field over the ocean", *J. Clim. Appl. Meteor.*, **22**, 1242-1252.

Hahn, D. G. and S. Manabe, 1975, "The role of the mountains in the south Asian monsoon circulation", *J. Atmos. Sci.*, **32**, 1515-1541.

Holopainen, E. O., 1970, "An observational study of the energy balance of the stationary disturbances in the atmosphere", *Quart. J. R. Met. Soc.*, **96**, 626-644.

Krishnamurti, T. N. and Kanamitsu, M., 1977, "Northern summer planetry-scale monsoons during drought and normal rainfall months", Monsoon Dynamics, ed. James Lighthill and Robert Pearce, pp. 19-48.

Ramage, C. S. and Raman, C. R. V., 1972, "Meteorological Atlas of the International Indian Ocean Expedition, vol. 2 : Upper air", National Science Foundation, Washington, D. C.

Saha, K. R. and Chang, C. P., 1983, "The baroclinic processes of monsoon depressions", *Mon. Weath. Rev.*, **111**, 1506-1514.

Saha, K. R. and Saha, S., 1989, "Vertical circulations and heat and moisture budgets in the time-mean July atmosphere over India and Bay of Bengal", *Mausam*, **40**, 159-168.